

**Supplementary Information for
Manganese Halide Hybrids for Reversible Luminous Color and
Application fro White Light-emitting Diode**

Hanmei Fu,^a Chunli Jiang,^{a,} Chunhua Luo,^a Hechun Lin,^a and Hui Peng^{a,b*}*

- a. Key Laboratory of Polar Materials and Devices (MOE), Department of Electronics, School of Physics and Electronic Science, East China Normal University, Shanghai, 200241, China. E-mail: cljiang@ee.ecnu.edu.cn; hpeng@ee.ecnu.edu.cn
- b. Collaborative Innovation Center of Extreme Optics, Shanxi University, Taiyuan, Shanxi 030006, China.

Table S1. Crystallographic data and structure refinements of $(C_5H_8N_2)_2MnCl_4$

Empirical formula	$(C_5H_8N_2)_2MnCl_4$	
Formula weight, g moL ⁻¹	389.01	
Crystal system	monoclinic	
Temperature, K	289 K	
Space group	<i>P</i> 2 ₁	
a, Å	13.3355 (6)	
b, Å	7.8283 (3)	
c, Å	16.6774 (8)	
Volume, Å ³	1738.81 (13)	
α, °	90	
β, °	92.888 (2)	
γ, °	90	
Z	4	
density, g·cm ⁻³	1.486	

Limiting indices	-15 ≤ h ≤ 15, -9 ≤ k ≤ 9, -19 ≤ l ≤ 19
$F(000)$	1024
Reflections collected	16899
Reflections unique	5996 [$R(\text{int}) = 0.0626$]
Completeness to $\theta = 66.715$, %	99.5
Refinement method	Full-matrix least-squares on F^2
Data/restraints/parameters	5996/1/347
Theta range for data collection, °	3.318 to 66.715
Goodness-of-fit on F^2	1.272
Absorption coefficient, mm^{-1}	11.769
Final R indices [$I > 2\delta(I)$]	$R_1 = 0.0702$, $wR_2 = 0.1735$
R indices (all data)	$R_1 = 0.0786$, $wR_2 = 0.1815$
Largest diff. peak and hole, e. Å ⁻³	0.564 and -1.586

Table S2. Anisotropic displacement parameters ($\text{\AA}^2 \times 10^3$) for $(\text{C}_5\text{H}_8\text{N}_2)_2\text{MnCl}_4$ at 289 K

	U^{11}	U^{22}	U^{33}	U^{23}	U^{13}	U^{12}
Mn1	24(1)	15(1)	27(1)	-1(1)	12(1)	-5(1)
Cl1	56(2)	59(2)	67(2)	-22(2)	36(2)	-43(2)
N1	56(6)	30(5)	38(5)	11(4)	0(4)	-11(5)
C1	44(6)	29(5)	50(7)	-4(5)	5(5)	-11(5)
Mn2	24(1)	17(1)	29(1)	1(1)	12(1)	-5(1)
Cl2	40(2)	27(1)	53(2)	5(1)	18(1)	10(1)
N2	32(5)	20(4)	48(6)	-8(4)	12(4)	-9(4)
C2	49(6)	20(4)	38(6)	0(4)	5(5)	10(4)
Cl3	49(2)	42(2)	37(2)	1(1)	-3(1)	-12(1)
N3	34(6)	184(16)	44(7)	-18(9)	6(5)	30(8)

C3	45(7)	16(5)	53(8)	-1(5)	-4(6)	2(4)
Cl4	43(2)	25(1)	52(2)	-4(1)	29(1)	1(1)
N4	28(5)	27(4)	39(5)	2(4)	9(4)	0(4)
C4	43(7)	56(7)	60(8)	2(7)	1(6)	2(6)
Cl5	44(2)	26(1)	48(2)	-7(1)	29(1)	0(1)
N5	22(4)	22(4)	29(5)	2(4)	6(3)	-3(4)
C5	61(9)	91(11)	60(9)	1(9)	16(7)	-3(8)
Cl6	50(2)	45(2)	40(2)	5(1)	-5(1)	-8(1)
N6	56(6)	29(5)	34(5)	-5(4)	18(4)	16(4)
C6	73(8)	5(4)	46(7)	3(4)	-8(6)	-6(5)
Cl7	41(2)	28(1)	49(2)	11(1)	14(1)	17(1)
N7	24(4)	18(4)	24(4)	0(3)	6(3)	0(3)
C7	31(6)	50(7)	36(6)	1(5)	13(5)	-29(5)
Cl8	54(2)	60(2)	66(2)	-18(2)	34(2)	-40(2)
N8	58(6)	31(5)	48(6)	6(5)	3(5)	12(4)
C8	51(7)	13(4)	35(6)	8(4)	4(5)	0(4)
C9	36(7)	76(10)	101(13)	-34(9)	32(7)	-6(7)
C10	88(12)	83(11)	82(11)	-22(9)	64(9)	-31(9)
C11	25(5)	50(6)	27(6)	4(5)	18(4)	11(5)
C12	38(6)	31(5)	45(7)	-2(5)	0(5)	-9(5)
C13	26(5)	31(5)	33(6)	0(5)	13(4)	-11(4)
C14	52(7)	28(5)	36(6)	-18(5)	15(5)	-14(5)
C15	50(7)	36(6)	81(10)	-32(7)	15(6)	-5(6)
C16	39(6)	19(4)	44(7)	3(5)	8(5)	-2(5)
C17	52(7)	14(4)	47(7)	-4(5)	-4(5)	-3(5)
C18	27(5)	26(5)	53(7)	-11(5)	7(5)	-6(4)

C19	46(6)	29(5)	30(6)	1(4)	-12(5)	-8(5)
C20	58(7)	20(5)	70(9)	-10(5)	-3(6)	9(5)

The anisotropic displacement factor exponent takes the form:

$$-2 \pi^2 [h^2 a^{*2} U^{11} + \dots + 2 h k a^* b^* U^{12}]$$

Table S3. The basic bond lengths (\AA) and angles ($^\circ$) of $(\text{C}_5\text{H}_8\text{N}_2)_2\text{MnCl}_4$ at 289 K

Mn1-Cl1	2.348 (3)	Cl1-Mn1-Cl3	111.03 (13)
Mn1-Cl2	2.371 (3)	Cl1-Mn1-Cl2	110.04 (14)
Mn1-Cl3	2.351 (3)	Cl3-Mn1-Cl2	111.82 (12)
Mn1-Cl4	2.369 (3)	Cl1-Mn1-Cl4	111.59 (11)
N1-C1	1.336 (14)	Cl3-Mn1-Cl4	108.04 (13)
N1-C2	1.405 (12)	Cl2-Mn1-Cl4	104.12 (11)
C1-N2	1.329 (13)	C1-N1-C2	110.3 (10)
C1-H1	0.9300	N1-C1-N2	107.4 (10)
Mn2-Cl8	2.346 (3)	N1-C1-H1	126.3
Mn2-Cl6	2.358 (3)	N2-C1-H1	126.3
Mn2-Cl5	2.363 (3)	Cl8-Mn2-Cl6	111.45 (13)
Mn2-Cl7	2.373 (3)	Cl8-Mn2-Cl5	111.80 (11)
N2-C3	1.359 (13)	Cl6-Mn2-Cl5	107.94 (13)
N2-C4	1.466 (13)	Cl8-Mn2-Cl7	110.06 (13)
C2-C3	1.355 (15)	Cl6-Mn2-Cl7	111.27 (11)
C2-H2	0.9300	Cl5-Mn2-Cl7	104.08 (11)
N3-C7	1.29 (2)	C1-N2-C3	108.9 (8)
N3-C8	1.356 (16)	C1-N2-C4	123.3 (10)
C3-H3	0.9300	C3-N2-C4	127.8 (10)
N4-C6	1.320 (13)	C3-C2-N1	103.5 (9)
N4-C8	1.384 (13)	C3-C2-H2	128.3

N4-C9	1.477 (12)	N1-C2-H2	128.3
C4-C5	1.448 (16)	C7-N3-C8	111.6 (11)
C4-H4A	0.9700	C2-C3-N2	109.9 (9)
C4-H4B	0.9700	C2-C3-H3	125.1
N5-C11	1.312 (11)	N2-C3-H3	125.1
N5-C13	1.378 (12)	C6-N4-C8	107.0 (8)
N5-C14	1.509 (13)	C6-N4-C9	129.8 (11)
C5-H5A	0.9600	C8-N4-C9	123.2 (10)
C5-H5B	0.9600	C5-C4-N2	111.1 (10)
C5-H5C	0.9600	C5-C4-H4A	109.5
N6-C11	1.292 (15)	N2-C4-H4A	109.5
N6-C12	1.375 (13)	C5-C4-H4B	109.3
C6-C7	1.227 (15)	N2-C4-H4B	109.4
C6-H6	0.9300	H4A-C4-H4B	108.0
N7-C16	1.320 (12)	C11-N5-C13	109.3 (9)
N7-C18	1.351 (12)	C11-N5-C14	125.9 (9)
N7-C19	1.449 (13)	C13-N5-C14	124.7 (8)
C7-H7	0.9300	C4-C5-H5A	109.5
N8-C17	1.362 (14)	C4-C5-H5B	109.4
N8-C16	1.372 (15)	H5A-C5-H5B	109.5
C8-H8	0.9300	C4-C5-H5C	109.5
C9-C10	1.44 (2)	H5A-C5-H5C	109.5
C9-H9A	0.9700	H5B-C5-H5C	109.5
C9-H9B	0.9700	C11-N6-C12	109.9 (9)
C10-H10A	0.9600	C7-C6-N4	111.8 (9)
C10-H10B	0.9600	C7-C6-H6	124.1

C10-H10C	0.9600	N4-C6-H6	124.1
C11-H11	0.9300	C16-N7-C18	109.7 (9)
C12-C13	1.320 (15)	C16-N7-C19	124.7 (9)
C12-H12	0.9300	C18-N7-C19	125.5 (9)
C13-H13	0.9300	C6-C7-N3	108.2 (10)
C14-C15	1.436 (17)	C6-C7-H7	125.9
C14-H14A	0.9700	N3-C7-H7	125.9
C14-H14B	0.9700	C17-N8-C16	107.0 (10)
C15-H15A	0.9600	N4-C8-N3	101.4 (10)
C15-H15B	0.9600	N4-C8-H8	129.3
C15-H15C	0.9600	N3-C8-H8	129.3
C16-H16	0.9300	C10-C9-N4	114.8 (13)
C17-C18	1.370 (15)	C10-C9-H9A	108.6
C17-H17	0.9300	N4-C9-H9A	108.6
C18-H18	0.9300	C10-C9-H9B	108.5
C19-C20	1.537 (14)	N4-C9-H9B	108.5
C19-H19A	0.9700	H9A-C9-H9B	107.5
C19-H19B	0.9700	C9-C10-H10A	109.5
C20-H20A	0.9600	C9-C10-H10B	109.4
C20-H20B	0.9600	H10A-C10-H10B	109.5
C20-H20C	0.9600	C9-C10-H10C	109.5
N7-C16-N8	108.3 (10)	H10A-C10-H10C	109.5
N7-C16-H16	125.8	H10B-C10-H10C	109.5
N8-C16-H16	125.8	N6-C11-N5	107.7 (10)
N8-C17-C18	107.9 (10)	N6-C11-H11	126.1
N8-C17-H17	126.1	N5-C11-H11	126.1

C18-C17-H17	126.1	C13-C12-N6	106.7 (9)
N7-C18-C17	106.9 (9)	C13-C12-H12	126.6
N7-C18-H18	126.5	N6-C12-H12	126.6
C17-C18-H18	126.5	C12-C13-N5	106.3 (9)
N7-C19-H19A	109.0	C12-C13-H13	126.9
C20-C19-H19A	109.0	N5-C13-H13	126.8
N7-C19-H19A	109.0	C15-C14-N5	111.7 (9)
C20-C19-H19A	109.0	C15-C14-H14A	109.3
H19A-C19-H19B	107.8	N5-C14-H14A	109.3
C19-C20-H20A	109.4	C15-C14-H14B	109.3
C19-C20-H20B	109.5	N5-C14-H14B	109.3
H20A-C20-H20B	109.5	H14A-C14-H14B	108.0
C19-C20-H20C	109.5	C14-C15-H15A	109.5
H20A-C20-H20C	109.5	C14-C15-H15B	109.5
H20B-C20-H20C	109.5	H15A-C15-H15B	109.5
H15B-C15-H15C	109.5	C14-C15-H15C	109.4
H15A-C15-H15C	109.5		

Symmetry transformations used to generate equivalent atoms:

#1 -x+1,-y,-z+1 #2 -x+2,-y+1,-z+1

Table S4. Hydrogen bond lengths and angles (\AA , $^\circ$) for C—H \cdots Cl interaction of $(\text{C}_5\text{H}_8\text{N}_2)_2\text{MnCl}_4$ at 289 K

D—H \cdots A	D—H	H \cdots A	D—A	$\angle D$ —H \cdots A
C7—H7 \cdots Cl4	0.9300	2.5440	3.2578	133.754
C17—H17 \cdots Cl5	0.9300	2.6630	3.5336	156.054
C9—H9A \cdots Cl7	0.9700	2.8270	3.7139	152.743
C4—H4B \cdots Cl2	0.9700	2.8320	3.7363	155.422

Table S5. The supporting information of these fabricated LEDs

Sample	R_m	Driven current (mA)	Chromaticity coordinate	CCT (K)
B	0:0	20	(0.1585, 0.0264)	1875
G	10:0	20	(0.2014, 0.5922)	8235
R	0:10	20	(0.6424, 0.3439)	9423
m1	2:3	20	(0.3529, 0.3615)	4748
m2	5:7	20	(0.3480, 0.3513)	4881
m3	3:4	20	(0.3444, 0.3389)	4971
m4	13:17	20	(0.3350, 0.3332)	5368
m5	9:11	20	(0.3242, 0.3277)	5896
m6	7:8	20	(0.3123, 0.3310)	6516
m4	13:17	50	(0.3222, 0.3353)	5982
m4	13:17	80	(0.3258, 0.3439)	5797
m4	13:17	110	(0.3308, 0.3462)	5573
m4	13:17	140	(0.3272, 0.3445)	5733
m'	11:13	20	(0.3245, 0.3159)	5902

R_m: mass ratio of (C₅H₈N₂)₂MnCl₄ and C₅H₈N₂(MnCl₂)_xCl_y phosphors.

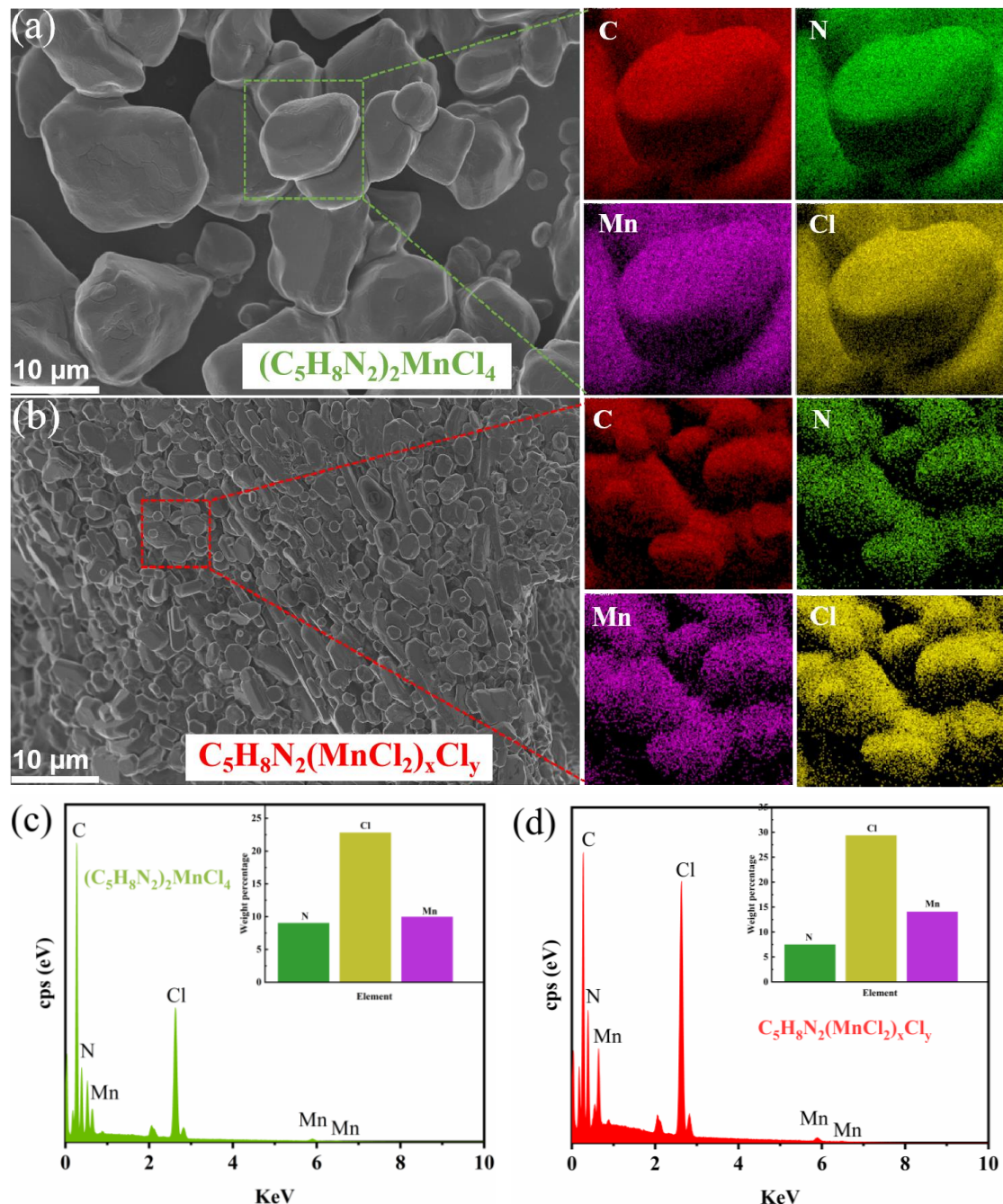


Fig. S1. The morphology and composition characterization of $(C_5H_8N_2)_2MnCl_4$ and $C_5H_8N_2(MnCl_2)_xCl_y$. (a) Scanning electron microscopy (SEM) and energy-dispersive X-ray spectroscopy (EDS) mapping images of $(C_5H_8N_2)_2MnCl_4$. (b) SEM image and EDS mapping images of $C_5H_8N_2(MnCl_2)_xCl_y$. (c) EDS spectrum of $(C_5H_8N_2)_2MnCl_4$. (d) EDS spectrum of $C_5H_8N_2(MnCl_2)_xCl_y$.

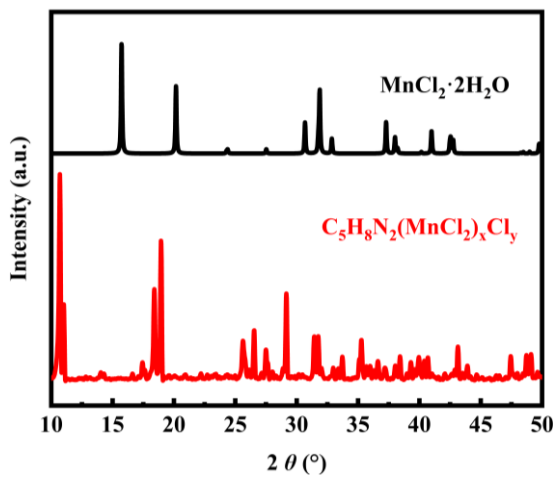


Fig. S2. The powder XRD patterns of $\text{MnCl}_2 \cdot 2\text{H}_2\text{O}$ and $\text{C}_5\text{H}_8\text{N}_2(\text{MnCl}_2)_x\text{Cl}_y$.

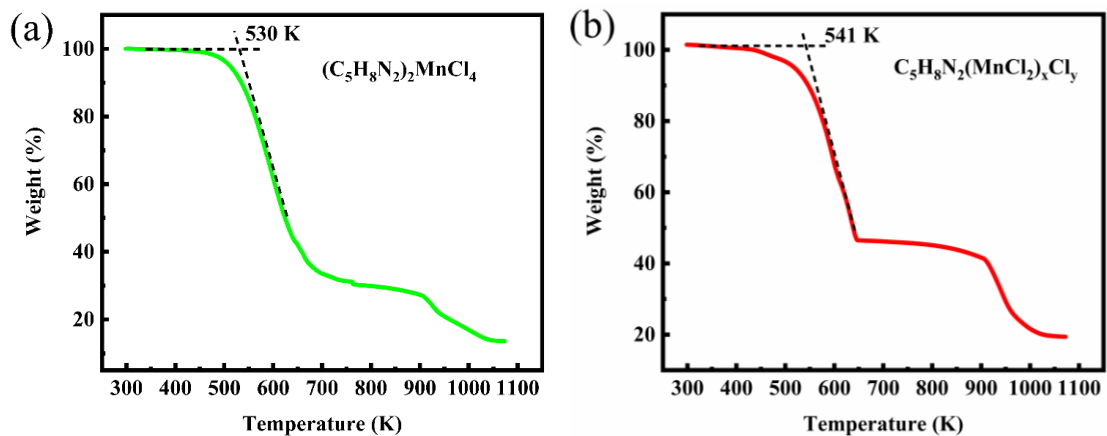


Fig. S3. Thermogravimetric analysis (TGA) patterns of $(\text{C}_5\text{H}_8\text{N}_2)_2\text{MnCl}_4$ (a) and $\text{C}_5\text{H}_8\text{N}_2(\text{MnCl}_2)_x\text{Cl}_y$ (b), indicating their good thermal stability.

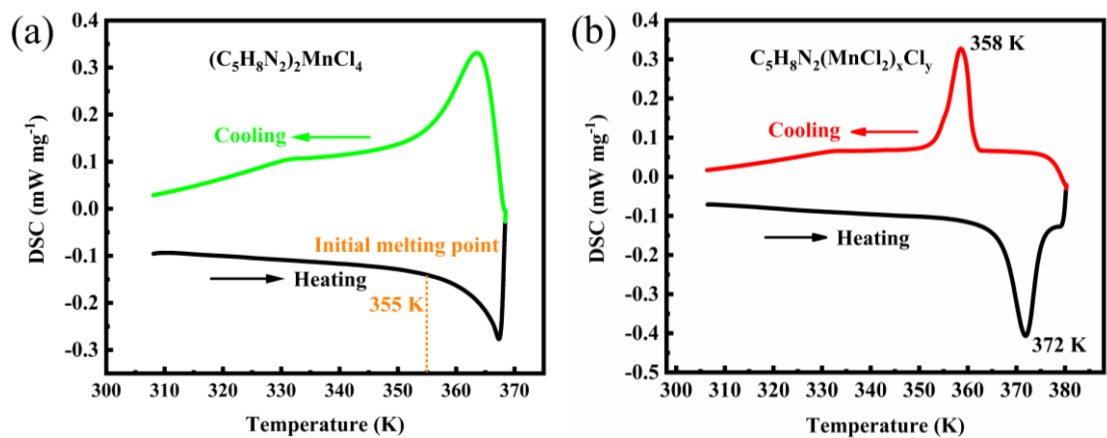


Fig. S4. The differential scanning calorimetry (DSC) patterns of $(\text{C}_5\text{H}_8\text{N}_2)_2\text{MnCl}_4$ (a) and $\text{C}_5\text{H}_8\text{N}_2(\text{MnCl}_2)_x\text{Cl}_y$ (b).

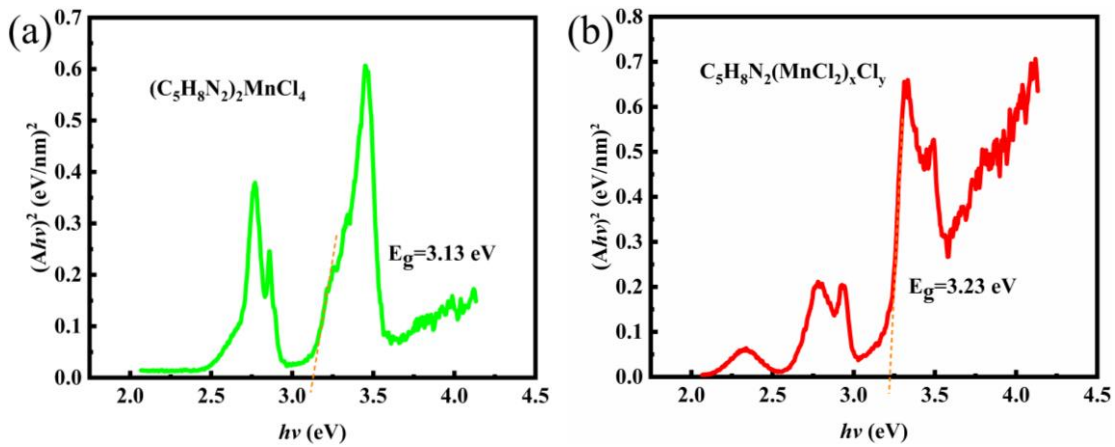


Fig. S5. The Tacu plots of $(\text{C}_5\text{H}_8\text{N}_2)_2\text{MnCl}_4$ (a) and $\text{C}_5\text{H}_8\text{N}_2(\text{MnCl}_2)_x\text{Cl}_y$ (b), showing the computative band gaps.

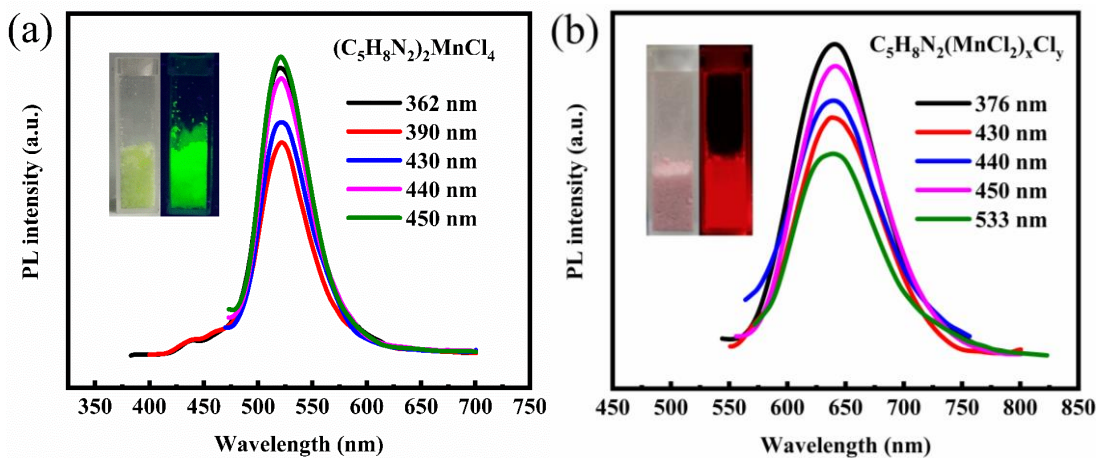


Fig. S6. Emission spectra of $(\text{C}_5\text{H}_8\text{N}_2)_2\text{MnCl}_4$ (a) and $\text{C}_5\text{H}_8\text{N}_2(\text{MnCl}_2)_x\text{Cl}_y$ (d) in ambient air, under different excitation wavelengths.

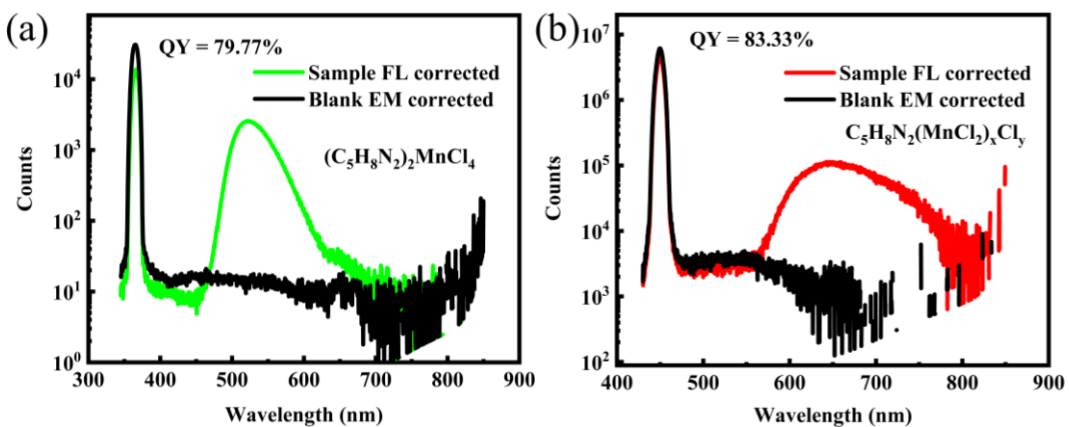


Fig. S7. Photoluminescence quantum yields (PLQYs) spectra of $(\text{C}_5\text{H}_8\text{N}_2)_2\text{MnCl}_4$ (a) and $\text{C}_5\text{H}_8\text{N}_2(\text{MnCl}_2)_x\text{Cl}_y$ (b), under the excitation wavelengths of 360 nm.

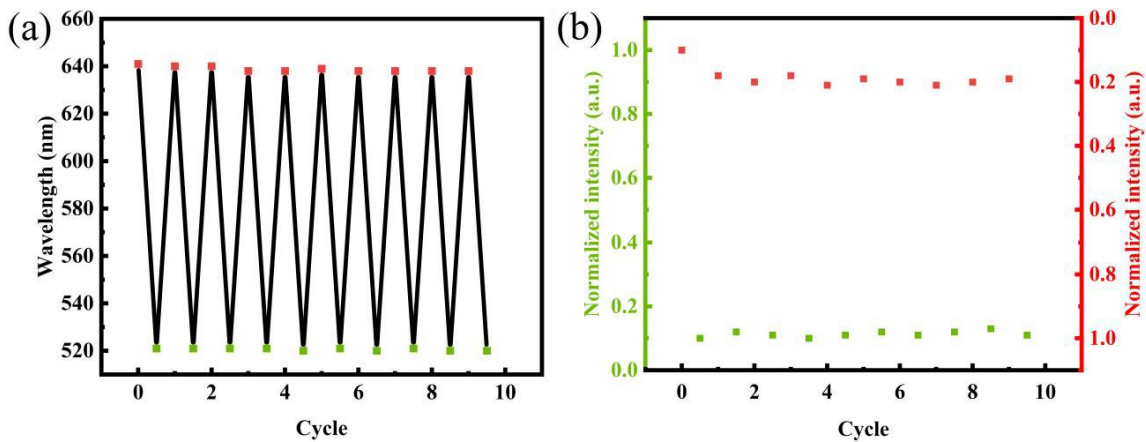


Fig. S8. The cyclic stability of luminescence conversion for $\text{C}_5\text{H}_8\text{N}_2(\text{MnCl}_2)_x\text{Cl}_y$ to $(\text{C}_5\text{H}_8\text{N}_2)_2\text{MnCl}_4$ indicated by emission peaks positions (a) and intensity (b) under different states. The red points represent $\text{C}_5\text{H}_8\text{N}_2(\text{MnCl}_2)_x\text{Cl}_y$ and green points present $(\text{C}_5\text{H}_8\text{N}_2)_2\text{MnCl}_4$.

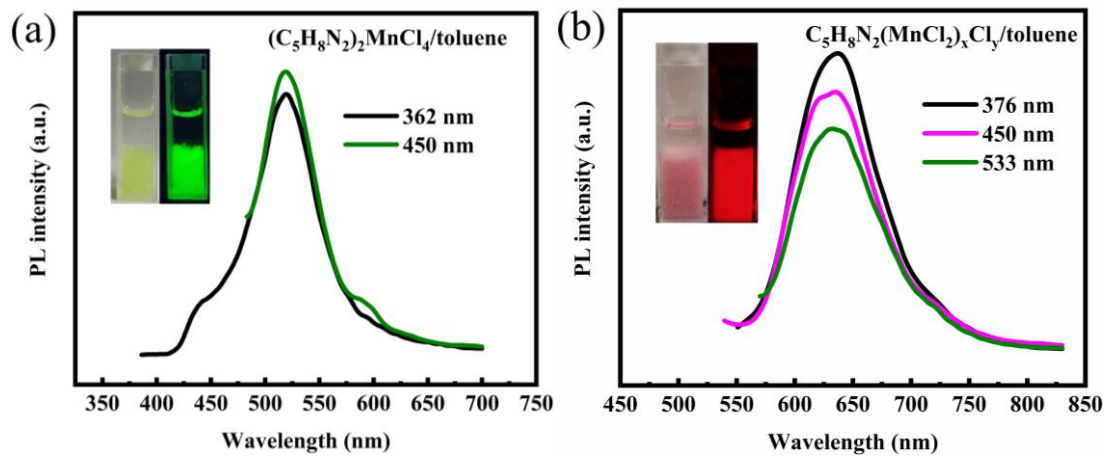


Fig. S9. Emission spectra of $(\text{C}_5\text{H}_8\text{N}_2)_2\text{MnCl}_4$ (a) and $\text{C}_5\text{H}_8\text{N}_2(\text{MnCl}_2)_x\text{Cl}_y$ (b) in toluene, under different excitation wavelengths.

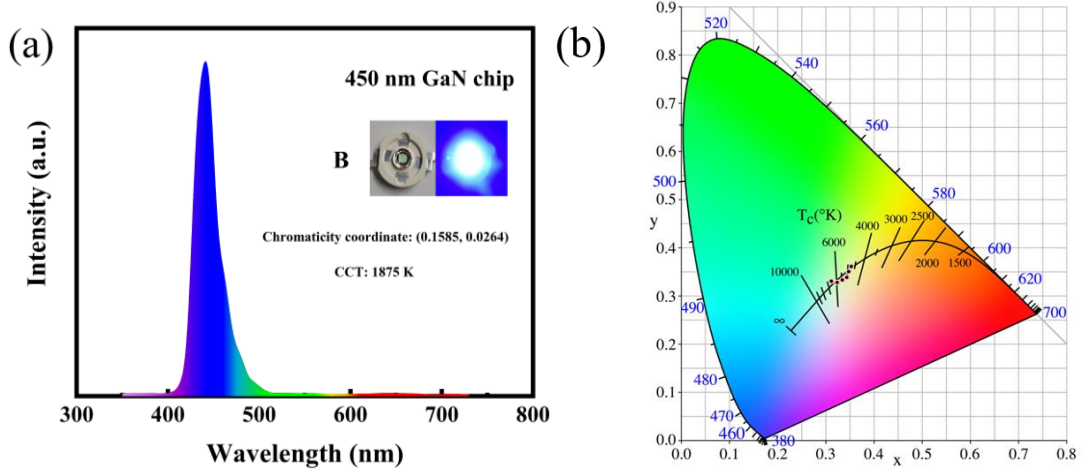


Fig. S10. (a) The emission spectrum of uncovered commercial 450 nm GaN blue LED (B). (b) The chromaticity diagram of the six WLED in Fig. S11.

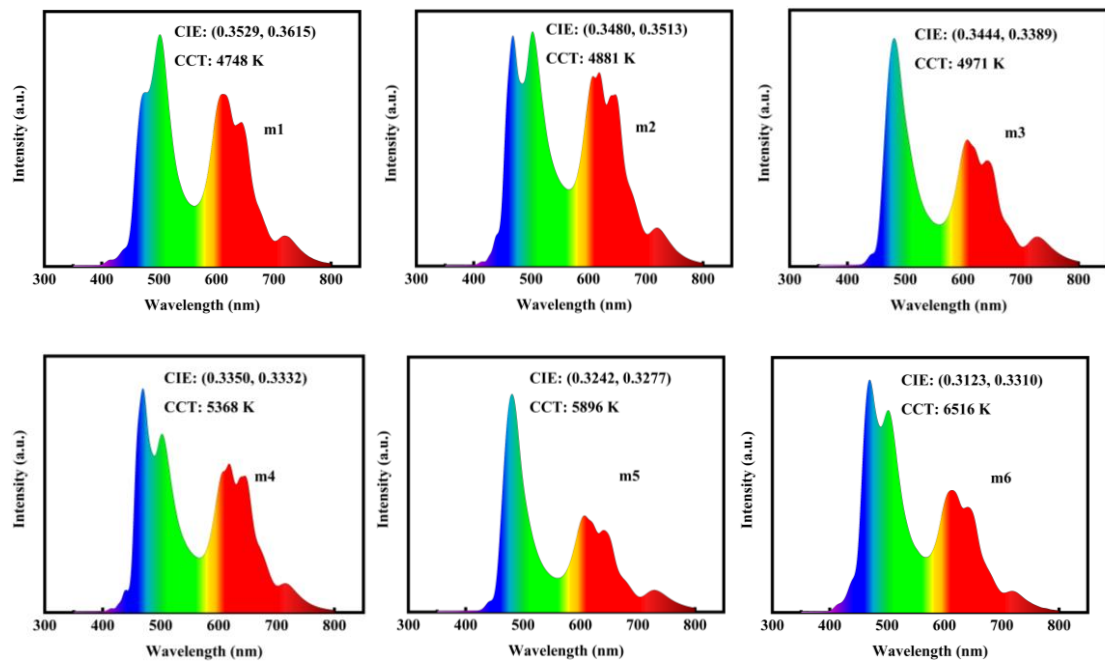


Fig. S11. The emission spectra of fabricated WLEDs ranging from neutral white to cold white.

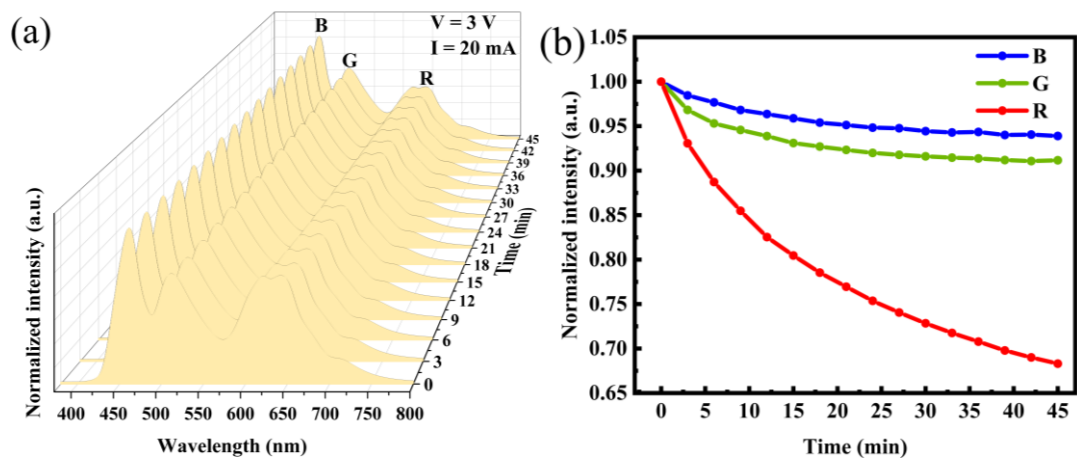


Fig. S12. The long-term stability of the fabricated WLED (m'), the emission spectra of fabricated WLED over time (a) and the change of emission intensity of the peaks (B, G, R) (b).